Contemporary Mathematics
Volume **548**, 2011

Use of random matrix theory for target detection, localization, and reconstruction

Josselin Garnier

Abstract. The detection, localization, and characterization of a target embedded in a medium is an important problem in wave sensor imaging. The responses between each pair of source and receiver are collected so that the available information takes the form of a response matrix between the source array and the receiver array. When the data are corrupted by additive noise we show how the target can be efficiently detected, localized and characterized using recent tools of random matrix theory.

1. Introduction

The detection, localization, and characterization of a target embedded in a medium is an important problem in wave sensor imaging [**8, 22**]. Sensor array imaging involves two steps. The first step is experimental, it consists in recording the waves generated by the sources and received by the sensors. The data set consists of a matrix of recorded signals whose indices are the index of the source and the index of the receiver. The second step is numerical, it consists in processing the recorded data in order to estimate some relevant features of the medium (reflector locations,...). The main applications of sensor array imaging are medical imaging, geophysical exploration, and non-destructive testing.

Recently it has been shown that random matrix theory could be used in order to build a detection test based on the statistical properties of the singular values of the response matrix [**9, 10, 11, 1, 2**]. This paper extends the results contained in [**1, 2**] into several important directions. First we address in this paper the case in which the source array and the receiver array are not coincident, and more generally the case in which the number of sources is different from the number of receivers. As a result the noise singular value distribution has the form of a deformed quarter circle and the statistics of the singular value associated to the target is also affected. Second we present a detailed analysis of the critical case when the singular value associated to the target is at the edge of the deformed

2000 *Mathematics Subject Classification.* 78A46, 15B52.
Key words and phrases. Imaging, random matrix theory.
This work was supported by National Institute for Mathematical Sciences (2010 Thematic Program, TP1003). We thank Habib Ammari, Hyeonbae Kang, and Knut Sølna for useful and stimulating discussions during the summer 2010 that we spent at Inha University.

quarter-circle distribution of the noise singular values. This analysis exhibits a new type of Tracy-Widom distribution. Third we study carefully the estimation of the noise variance of the response matrix. Different estimators are studied and an estimator that achieves the optimal trade-off between bias and variance is proposed. The use of this estimator instead of the empirical estimator used in the previous versions significantly improves the quality of the detection test based on the singular value distribution of the measured response matrix when the number of sensors is not very large. Fourth we propose an algorithm that can reconstruct not only the position of the target, but its scattering amplitude. The estimator of the scattering amplitude compensates for the level repulsion of the singular value associated to the target due to the noise and it is much better than the empirical estimator.

2. The Response Matrix

We address the case of a point reflector that can model a small dielectric anomaly in electromagnetism, a small density anomaly in acoustics, or more generally a local variation of the index of refraction in the scalar wave equation. The contrast of the anomaly can be of order one but its volume is small compared to the wavelength. In such a situation it is possible to expand the solution of the wave equation around the background solution [**3, 4, 5, 6**].

Let us consider the scalar wave equation in a d-dimensional homogeneous medium with the index of refraction n_0. The reference speed of propagation is denoted by c. We assume that the target is a small reflector or inclusion D with the index of refraction $n_{\rm ref} \neq n_0$. The support of the inclusion is of the form $D = \boldsymbol{x}_{\rm ref} + B$, where B is a domain with small volume. Therefore the scalar wave equation with the source $S(t,x)$ takes the form

$$\frac{n^2(\boldsymbol{x})}{c^2}\partial_t^2 E - \Delta_{\boldsymbol{x}} E = S(t,\boldsymbol{x}),$$

where the index of refraction is given by

$$n(\boldsymbol{x}) = n_0 + (n_{\rm ref} - n_0)\mathbf{1}_D(\boldsymbol{x}).$$

For any $\boldsymbol{y}_n, \boldsymbol{z}_m$ far from $\boldsymbol{x}_{\rm ref}$ the field $\mathrm{Re}(\hat{E}(\boldsymbol{y}_n,\boldsymbol{z}_m)e^{-i\omega t})$ observed at $\boldsymbol{y}_n$ when a point source emits a time-harmonic signal with frequency ω at $\boldsymbol{z}_m$ can be expanded as powers of the volume as

$$\hat{E}(\boldsymbol{y}_n,\boldsymbol{z}_m) = \hat{G}(\boldsymbol{y}_n,\boldsymbol{z}_m) + k_0^2\rho_{\rm ref}\hat{G}(\boldsymbol{y}_n,\boldsymbol{x}_{\rm ref})\hat{G}(\boldsymbol{x}_{\rm ref},\boldsymbol{z}_m) + O(|B|^{\frac{d+1}{d}}), \tag{2.1}$$

where $k_0 = n_0\omega/c$ is the homogeneous wavenumber, $\rho_{\rm ref}$ is the scattering amplitude

$$\rho_{\rm ref} = \Big(\frac{n_{\rm ref}^2}{n_0^2} - 1\Big)|B|, \tag{2.2}$$

and $\hat{G}(\boldsymbol{x},\boldsymbol{z})$ is the Green's function or fundamental solution of the Helmholtz equation with a point source at $\boldsymbol{z}$:

$$\Delta_{\boldsymbol{x}}\hat{G}(\boldsymbol{x},\boldsymbol{z}) + k_0^2\hat{G}(\boldsymbol{x},\boldsymbol{z}) = -\delta(\boldsymbol{x}-\boldsymbol{z}). \tag{2.3}$$

More explicitly we have

$$\hat{G}(\boldsymbol{x},\boldsymbol{z}) = \begin{cases} \dfrac{i}{4}H_0^{(1)}(k_0|\boldsymbol{x}-\boldsymbol{z}|) & \text{if } d=2, \\ \dfrac{e^{ik_0|\boldsymbol{x}-\boldsymbol{z}|}}{4\pi|\boldsymbol{x}-\boldsymbol{z}|} & \text{if } d=3, \end{cases}$$

where $H_0^{(1)}$ is the Hankel function of the first kind of order zero.

When there are M sources $(\boldsymbol{z}_m)_{m=1,\dots,M}$ and N receivers $(\boldsymbol{y}_n)_{n=1,\dots,N}$, the response matrix is the $N \times M$ matrix $\mathbf{A}_0 = (A_{0nm})_{n=1,\dots,N,m=1,\dots,M}$ defined by

$$A_{0nm} := \hat{E}(\boldsymbol{y}_n, \boldsymbol{z}_m) - \hat{G}(\boldsymbol{y}_n, \boldsymbol{z}_m) \tag{2.4}$$

This matrix has rank one:

$$\mathbf{A}_0 = \sigma_{\text{ref}} \boldsymbol{u}_{\text{ref}} \boldsymbol{v}_{\text{ref}}^{\dagger}, \tag{2.5}$$

where † stands for the conjugate transpose. The nonzero singular value is

$$\sigma_{\text{ref}} = k_0^2 \rho_{\text{ref}} \big(\sum_{l=1}^{N} |\hat{G}(\boldsymbol{y}_l, \boldsymbol{x})|^2 \big)^{1/2} \big(\sum_{l=1}^{M} |\hat{G}(\boldsymbol{z}_l, \boldsymbol{x})|^2 \big)^{1/2}. \tag{2.6}$$

The associated left and right singular vectors $\boldsymbol{u}_{\text{ref}}$ and $\boldsymbol{v}_{\text{ref}}$ are given by:

$$\boldsymbol{u}_{\text{ref}} = \boldsymbol{u}(\boldsymbol{x}_{\text{ref}}), \qquad \boldsymbol{v}_{\text{ref}} = \boldsymbol{v}(\boldsymbol{x}_{\text{ref}}), \tag{2.7}$$

where we have defined the normalized vectors of Green's functions:

$$\boldsymbol{u}(\boldsymbol{x}) = \Big(\frac{\hat{G}(\boldsymbol{y}_n, \boldsymbol{x})}{\big(\sum_{l=1}^{N} |\hat{G}(\boldsymbol{y}_l, \boldsymbol{x})|^2 \big)^{1/2}} \Big)_{n=1,\dots,N}, \tag{2.8}$$

$$\boldsymbol{v}(\boldsymbol{x}) = \Big(\frac{\overline{\hat{G}(\boldsymbol{z}_m, \boldsymbol{x})}}{\big(\sum_{l=1}^{M} |\hat{G}(\boldsymbol{z}_l, \boldsymbol{x})|^2 \big)^{1/2}} \Big)_{m=1,\dots,M}. \tag{2.9}$$

The matrix $\mathbf{A}_0$ is the complete data set that can be collected. In practice the measured matrix is corrupted by electronic or measurement noise that has the form of an additive noise. The purpose of imaging is to answer the following questions given the data set:

- is there a target in the medium ? This is the detection problem. In the absence of noise this question is trivial in that we can claim that there is a target buried in the medium as soon as the response matrix is not zero. In the presence of noise, it is not so obvious to answer this question since the response matrix is not zero due to additive noise even in the absence of a target. Our purpose is to build a detection test that has the maximal probability of detection for a given false alarm rate.
- where is the target ? This is the localization problem. Several methods can be proposed, essentially based on the back-propagation of the data set, and we will describe which methods are the most robust in the presence of noise.
- what are the characteristic properties of the target ? This is the reconstruction problem. One may look after geometric and physical properties. In fact, in view of the expression (2.1), only the product of the volume of the inclusion times the contrast can be identified in the regime we address in this paper.

The paper is organized as follows. In Section 3 we explain how the data should be collected to minimize the impact of the additive noise. In Section 4 we give known and new results about the distribution of the singular values of the response matrix, with special emphasis on the largest singular value. In Section 5 we discuss how the noise level can be estimated with minimal bias and variance. In Section 6 we build a test for the detection of the target and in Section 7 we show how the position and the scattering amplitude of the target can be estimated.

3. Data Acquisition

In this section we consider that there are M sources and N receivers. The measures are noisy, which means that the signal measured by a receiver is corrupted by an additive noise that can be described in terms of a complex Gaussian random variable with mean zero and variance $\sigma_{\rm n}^2$ (in other words, the real and imaginary parts of the measurement noise are independent and follow a Gaussian distribution with mean zero and variance $\sigma_{\rm n}^2/2$). The recorded noises are independent from each other.

3.1. Standard Acquisition. In the standard acquisition scheme, the response matrix is measured during a sequence of M experiments. In the mth experience, $m=1,\ldots,M$, the mth source (located at $\boldsymbol{z}_m$) generates a time-harmonic signal with unit amplitude and the N receivers (located at $\boldsymbol{y}_n$, $n=1,\ldots,N$) record the backscattered waves which means that they measure

$$A_{{\rm meas},nm} = A_{0,nm} + W_{nm}, \quad n=1,\ldots,N, \quad m=1,\ldots,M,$$

which gives the matrix

$$\mathbf{A}_{\rm meas} = \mathbf{A}_0 + \mathbf{W}, \tag{3.1}$$

where $\mathbf{A}_0$ is the unperturbed response matrix of rank one (2.4) and W_{nm} are independent complex Gaussian random variables with mean zero and variance $\sigma_{\rm n}^2$.

3.2. Optimal Acquisition: Hadamard Technique. The Hadamard technique is a noise reduction technique in the presence of additive noise that uses the structure of Hadamard matrices.

Definition 3.1. A real Hadamard matrix $\mathbf{H}$ of order M is a $M\times M$ matrix whose elements are -1 or $+1$ and such that $\mathbf{H}^T\mathbf{H} = M\mathbf{I}$. Here T stands for the transpose.

Real Hadamard matrices do not exist for all M. A necessary condition for the existence is that $M=1,2$ or a multiple of 4. A sufficient condition is that M is a power of two. Explicit examples are known for all M multiple of 4 up to $M=664$ [**20**]. The Hadamard conjecture proposes that a Hadamard matrix of order $4k$ exists for every positive integer k.

Definition 3.2. A complex Hadamard matrix $\mathbf{H}$ of order M is a $M\times M$ matrix whose elements are of modulus one and such that $\mathbf{H}^\dagger\mathbf{H} = M\mathbf{I}$. Here $\dagger$ stands for the conjugate transpose.

Complex Hadamard matrices exist for all M. For instance the Fourier matrix

$$H_{nm} = \exp\Big[i2\pi\frac{(n-1)(m-1)}{M}\Big], \qquad m,n=1,\ldots,M, \tag{3.2}$$

is a complex Hadamard matrix.

A Hadamard matrix has maximal determinant among matrices with complex entries in the closed unit disk. More exactly Hadamard [**16**] proved that the determinant of any complex $M\times M$ matrix $\mathbf{H}$ with entries in the closed unit disk satisfies $|\det\mathbf{H}| \le M^{M/2}$, with equality attained by a complex Hadamard matrix.

We now describe a general multi-source acquisition scheme and show the importance of Hadamard matrices to build an optimal scheme. Let $\mathbf{H}$ be an invertible $M\times M$ matrix with complex entries in the closed unit disk. In the multi-source

acquisition scheme, the response matrix is measured during a sequence of M experiments. In the mth experience, $m = 1, \dots, M$, all sources generate unit amplitude time harmonic signals, the m' source generating $H_{m'm}$. This means that we use all sources to their maximal emission capacity with a specific coding of their phases. The N receivers record the backscattered waves which means that they measure

$$B_{\mathrm{meas},nm} = \sum_{m'=1}^{M} H_{m'm} A_{0,nm'} + W_{nm} = (\mathbf{A}_0 \mathbf{H})_{nm} + W_{nm}, \qquad n = 1, \dots, N.$$

Collecting the recorded signals of the $m = 1, \dots, M$ experiments gives the matrix

$$\mathbf{B}_{\mathrm{meas}} = \mathbf{A}_0 \mathbf{H} + \mathbf{W},$$

where $\mathbf{A}_0$ is the unperturbed response matrix and W_{nm} are independent complex Gaussian random variables with mean zero and variance σ_{n}^2. The measured response matrix $\mathbf{A}_{\mathrm{meas}}$ is obtained by right multiplying the matrix $\mathbf{B}_{\mathrm{meas}}$ by the matrix $\mathbf{H}^{-1}$:

$$\mathbf{A}_{\mathrm{meas}} := \mathbf{B}_{\mathrm{meas}} \mathbf{H}^{-1} = \mathbf{A}_0 \mathbf{H} \mathbf{H}^{-1} + \mathbf{W} \mathbf{H}^{-1}, \tag{3.3}$$

so that we get the unperturbed matrix $\mathbf{A}_0$ up to a new noise

$$\mathbf{A}_{\mathrm{meas}} = \mathbf{A}_0 + \widetilde{\mathbf{W}}, \qquad \widetilde{\mathbf{W}} = \mathbf{W} \mathbf{H}^{-1}. \tag{3.4}$$

The choice of the matrix $\mathbf{H}$ should fulfill the property that the new noise matrix $\widetilde{\mathbf{W}}$ has independent complex entries with Gaussian statistics, mean zero, and minimal variance. We have

$$\begin{aligned}
\mathbb{E}\Big[\overline{\widetilde{W}_{nm}} \widetilde{W}_{n'm'}\Big] &= \sum_{q,q'=1}^{M} \overline{(\mathbf{H}^{-1})_{qm}} (\mathbf{H}^{-1})_{q'm'} \mathbb{E}\big[\overline{W_{nq}} W_{n'q'}\big] \\
&= \sigma_{\mathrm{n}}^2 \sum_{q,q'=1}^{M} \overline{(\mathbf{H}^{-1})_{qm}} (\mathbf{H}^{-1})_{q'm'} \mathbf{1}_n(n') \mathbf{1}_q(q') \\
&= \sigma_{\mathrm{n}}^2 \sum_{q=1}^{M} ((\mathbf{H}^{-1})^\dagger)_{mq} (\mathbf{H}^{-1})_{qm'} \mathbf{1}_n(n') \\
&= \sigma_{\mathrm{n}}^2 ((\mathbf{H}^{-1})^\dagger \mathbf{H}^{-1})_{mm'} \mathbf{1}_n(n'),
\end{aligned}$$

where $\mathbb{E}$ stands for the expectation. This shows that we look for a complex matrix $\mathbf{H}$ with entries in the unit disk such that $(\mathbf{H}^{-1})^\dagger \mathbf{H}^{-1} = c\mathbf{I}$ with a minimal c. This is equivalent to require that $\mathbf{H}$ is unitary and that $|\det \mathbf{H}|$ is maximal. Using Hadamard result we know that the maximal determinant is $M^{M/2}$ and that a complex Hadamard matrix attains the maximum. Therefore the optimal matrix $\mathbf{H}$ that minimizes the noise variance should be a Hadamard matrix, such as, for instance, the Fourier matrix (3.2). Note that, in the case of a linear array, the use of a Fourier matrix corresponds to an illumination in the form of plane waves with regularly sampled angles.

When the multi-source acquisition scheme is used with a Hadamard technique, we have $\mathbf{H}^{-1} = \frac{1}{M} \mathbf{H}^\dagger$ and the new noise matrix $\widetilde{\mathbf{W}}$ in (3.4) has independent complex entries with Gaussian statistics, mean zero, and variance $\sigma_{\mathrm{n}}^2 / M$:

$$\mathbb{E}\Big[\overline{\widetilde{W}_{nm}} \widetilde{W}_{n'm'}\Big] = \frac{\sigma_{\mathrm{n}}^2}{M} \mathbf{1}_m(m') \mathbf{1}_n(n'). \tag{3.5}$$

This gain of a factor M in the signal-to-noise ratio is called the Hadamard advantage.

4. Singular Value Decomposition of the Response Matrix

4.1. Singular Values of a Noisy Matrix. We consider here the situation in which the measured response matrix consists of independent noise coefficients with mean zero and variance $\sigma_{\rm n}^2/M$ and the number of receivers is larger than the number of sources $N \geq M$. This is the case when the response matrix is acquired with the Hadamard technique and there is no target in the medium.

We denote by $\sigma_1^{(M)} \geq \sigma_2^{(M)} \geq \sigma_3^{(M)} \geq \cdots \geq \sigma_M^{(M)}$ the singular values of the response matrix $\mathbf{A}$ sorted by decreasing order and by $\Lambda^{(M)}$ the corresponding integrated density of states defined by

$$\Lambda^{(M)}([a,b]) := \frac{1}{M}\mathrm{Card}\left\{l = 1,\ldots,M\,,\ \sigma_l^{(M)} \in [a,b]\right\}, \qquad \text{for any } a < b.$$

$\Lambda^{(M)}$ is a counting measure which consists of a sum of Dirac masses:

$$\Lambda^{(M)} = \frac{1}{M}\sum_{j=1}^{M} \delta_{\sigma_j^{(M)}}.$$

For large N and M with $N/M = \gamma \geq 1$ fixed we have the following results.

PROPOSITION 4.1. a) *The random measure $\Lambda^{(M)}$ almost surely converges to the deterministic absolutely continuous measure Λ with compact support:*

$$\Lambda([\sigma_u,\sigma_v]) = \int_{\sigma_u}^{\sigma_v} \frac{1}{\sigma_{\rm n}}\rho_\gamma\Big(\frac{\sigma}{\sigma_{\rm n}}\Big)d\sigma, \qquad 0 \leq \sigma_u \leq \sigma_v \tag{4.1}$$

where ρ_γ is the deformed quarter-circle law given by

$$\rho_\gamma(x) = \begin{cases} \dfrac{1}{\pi\sigma x}\sqrt{\big((\gamma^{1/2}+1)^2 - x^2\big)\big(x^2 - (\gamma^{1/2}-1)^2\big)} & \text{if } \gamma^{1/2}-1 < x \leq \gamma^{1/2}+1, \\ 0 & \text{otherwise.} \end{cases} \tag{4.2}$$

b) *The normalized l^2-norm of the singular values satisfies*

$$M\Big[\frac{1}{M}\sum_{j=1}^{M}(\sigma_j^{(M)})^2 - \gamma\sigma_{\rm n}^2\Big] \overset{M\to\infty}{\longrightarrow} \sqrt{\gamma}\sigma_{\rm n}^2 Z_0 \text{ in distribution,} \tag{4.3}$$

where Z_0 follows a Gaussian distribution with mean zero and variance one.

c) *The maximal singular value satisfies*

$$\sigma_1^{(M)} \simeq \sigma_{\rm n}\Big[\gamma^{1/2} + 1 + \frac{1}{2M^{2/3}}\big(1+\gamma^{-1/2}\big)^{1/3} Z_2 + o\big(\frac{1}{M^{2/3}}\big)\Big] \text{ in distribution,} \tag{4.4}$$

where Z_2 follows a type-2 Tracy Widom distribution.

The type-2 Tracy-Widom distribution has the cdf $\Phi_{\rm TW2}$ given by

$$\Phi_{\rm TW2}(z) = \exp\Big(-\int_z^\infty (x-z)\varphi^2(x)dx\Big),$$

where $\varphi(x)$ is the solution of the Painlevé equation

$$\varphi''(x) = x\varphi(x) + 2\varphi(x)^3, \quad \varphi(x) \simeq \mathrm{Ai}(x),\ x \to \infty, \tag{4.5}$$

Ai being the Airy function. The expectation of Z_2 is $\mathbb{E}[Z_2] \simeq -1.77$ and its variance is $\mathrm{Var}(Z_2) \simeq 0.81$. Detailed results about the Tracy-Widom distributions can be found in [**13**].

PROOF. Point a) is Marcenko-Pastur result [**18**]. Point b) follows from the expression of the normalized l^2-norm of the singular values in terms of the entries of the matrix:

$$\frac{1}{M}\sum_{j=1}^{M}(\sigma_j^{(M)})^2 = \frac{1}{M}\mathrm{Tr}\big(\mathbf{A}^\dagger\mathbf{A}\big) = \frac{1}{M}\sum_{n=1}^{N}\sum_{m=1}^{M}|A_{nm}|^2,$$

and from the application of the central limit theorem in the regime $M \gg 1$. The third point follows from [**17**]. □

4.2. Singular Values of the Perturbed Response Matrix. The response matrix using the Hadamard technique in the presence of a target and in the presence of measurement noise is

$$\mathbf{A} = \mathbf{A}_0 + \mathbf{W}, \tag{4.6}$$

where $\mathbf{A}_0$ is given by (2.4) and $\mathbf{W}$ has independent random complex entries with Gaussian statistics, mean zero and variance σ_{n}^2/M.

We consider the critical regime in which the singular values of the unperturbed matrix are of the same order as the singular values of the noise, that is to say, σ_{ref} is of the same order of magnitude as σ_{n}. We will say a few words about the cases σ_{ref} much larger or much smaller than σ_{n} after the analysis of the critical regime.

PROPOSITION 4.2. *In the regime $M \to \infty$:*

a) *The normalized l^2-norm of the singular values satisfies*

$$M\Big[\frac{1}{M}\sum_{j=1}^{M}(\sigma_j^{(M)})^2 - \gamma\sigma_{\mathrm{n}}^2\Big] \overset{M\to\infty}{\longrightarrow} \sigma_{\mathrm{ref}}^2 + \sqrt{2\gamma}\sigma_{\mathrm{n}}^2 Z_0 \text{ in distribution,} \tag{4.7}$$

where Z_0 follows a Gaussian distribution with mean zero and variance one.

b1) *If $\sigma_{\mathrm{ref}} < \gamma^{1/4}\sigma_{\mathrm{n}}$, then the maximal singular value satisfies*

$$\sigma_1^{(M)} \simeq \sigma_{\mathrm{n}}\Big[\gamma^{1/2} + 1 + \frac{1}{2M^{2/3}}\big(1+\gamma^{-1/2}\big)^{1/3}Z_2 + o(\frac{1}{M^{2/3}})\Big] \text{ in distribution,} \tag{4.8}$$

where Z_2 follows a type-2 Tracy Widom distribution.

b2) *If $\sigma_{\mathrm{ref}} = \gamma^{1/4}\sigma_{\mathrm{n}}$, then the maximal singular value satisfies*

$$\sigma_1^{(M)} \simeq \sigma_{\mathrm{n}}\Big[\gamma^{1/2} + 1 + \frac{1}{2M^{2/3}}\big(1+\gamma^{-1/2}\big)^{1/3}Z_3 + o(\frac{1}{M^{2/3}})\Big] \text{ in distribution,} \tag{4.9}$$

where Z_3 follows a type-3 Tracy Widom distribution.

b3) *If $\sigma_{\mathrm{ref}} > \gamma^{1/4}\sigma_{\mathrm{n}}$, then the maximal singular value has Gaussian distribution with the mean and variance given by*

$$\mathbb{E}\big[\sigma_1^{(M)}\big] = \sigma_{\mathrm{ref}}\Big[\Big(1 + (1+\gamma)\frac{\sigma_{\mathrm{n}}^2}{\sigma_{\mathrm{ref}}^2} + \gamma\frac{\sigma_{\mathrm{n}}^4}{\sigma_{\mathrm{ref}}^4}\Big)^{1/2} + o(\frac{1}{M^{1/2}})\Big], \tag{4.10}$$

$$\mathrm{Var}\big(\sigma_1^{(M)}\big) = \frac{\sigma_{\mathrm{n}}^2}{2M}\Big[\frac{1-\gamma\frac{\sigma_{\mathrm{n}}^4}{\sigma_{\mathrm{ref}}^4}}{\big(1+(1+\gamma)\frac{\sigma_{\mathrm{n}}^2}{\sigma_{\mathrm{ref}}^2}+\gamma\frac{\sigma_{\mathrm{n}}^4}{\sigma_{\mathrm{ref}}^4}\big)^{1/2}} + o(1)\Big]. \tag{4.11}$$

The type-3 Tracy-Widom distribution has the cdf $\Phi_{\rm TW3}$ given by

$$\Phi_{\rm TW3}(z) = \exp\Big(- \int_z^\infty \varphi(x) + (x-z)\varphi^2(x) dx \Big).$$

The expectation of Z_3 is $\mathbb{E}[Z_3] \simeq -0.49$ and its variance is $\mathrm{Var}(Z_3) \simeq 1.22$.

PROOF. Point a follows again from the explicit expression of the l^2-norm of the singular values in terms of the entries of the matrix. Point b in the case $N = M$ is addressed in [**14**] and the extension to $N \geq M$ is only technical. □

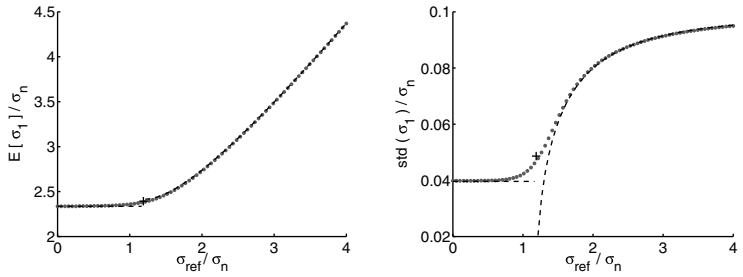

FIGURE 1. Mean and standard deviation of the first singular value. We compare the empirical means (left) and standard deviations (right) obtained from 10^4 MC simulations (blue dots) with the theoretical formulas given in Proposition 4.2 (dashed lines for the cases $\sigma_{\rm ref}/\sigma_{\rm n} < \gamma^{1/4}$ and $\sigma_{\rm ref}/\sigma_{\rm n} > \gamma^{1/4}$, crosses for the case $\sigma_{\rm ref}/\sigma_{\rm n} = \gamma^{1/4}$). Here $N = 100$ and $M = 50$ ($\gamma = 2$).

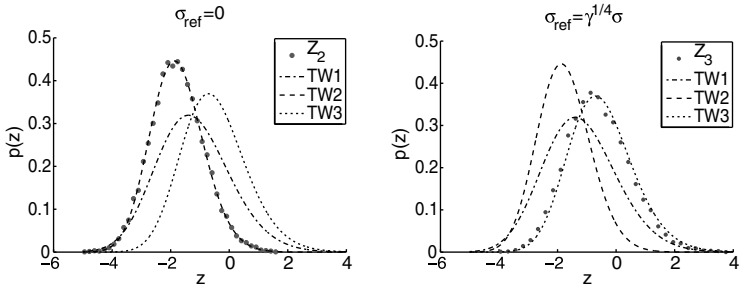

FIGURE 2. Histogram of the normalized first singular value. We plot the histogram of $2M^{1/3}(\sigma_1^{(M)}/\sigma_{\rm n} - \gamma^{1/2} - 1)/(1+\gamma^{-1/2})^{1/3}$ when $\sigma_{\rm ref} = 0$ (left) and when $\sigma_{\rm ref} = \gamma^{1/4}\sigma_{\rm n}$ (right). The histograms are evaluated from 10^4 MC simulations and compare with the densities of the theoretical Tracy-Widom distributions of type 1, 2, and 3. Here $N = 100$ and $M = 50$ ($\gamma = 2$).

Note that formula (4.11) seems to predict that the variance of the maximal singular value cancels when $\sigma_{\rm ref} \searrow \gamma^{1/4}\sigma_{\rm n}$, but this is true only to the order M^{-1}.

Formula (4.9) gives the exact distribution of the maximal singular value when $\sigma_{\rm ref} = \gamma^{1/4}\sigma_{\rm n}$, whose variance is of order $M^{-4/3}$:

$$\mathrm{Var}\big(\sigma_1^{(M)}\big) = \frac{\sigma_{\rm n}^2\big(1+\gamma^{-1/2}\big)^{2/3}}{4M^{4/3}}\mathrm{Var}(Z_3) + o\big(\frac{1}{4M^{4/3}}\big). \tag{4.12}$$

Following [**12**] we can anticipate that there are interpolating distributions which appear when

$$\sigma_{\rm ref} = \gamma^{1/4}\sigma_{\rm n} + \frac{w}{M^{1/3}}.$$

These distributions should be modified type-3 distributions when $w \neq 0$. We will not study this problem in this paper.

4.3. Singular Vectors of the Perturbed Response Matrix. It is of interest to describe the statistical distribution of the angles between the first left and right singular vectors $\boldsymbol{u}_1^{(M)}$ and $\boldsymbol{v}_1^{(M)}$ of the noisy matrix $\mathbf{A}$ with respect to the first left and right singular vectors $\boldsymbol{u}_{\rm ref}$ and $\boldsymbol{v}_{\rm ref}$ of the unperturbed matrix $\mathbf{A}_0$. This plays a role in the MUSIC (MUltiple SIgnal Classification) algorithm that we discuss in Section 7.1. In the following $\langle \boldsymbol{u}, \boldsymbol{v}\rangle$ stands for the scalar product $\boldsymbol{u}^\dagger\boldsymbol{v}$.

PROPOSITION 4.3. *In the regime $M \to \infty$:*

a) *If $\sigma_{\rm ref} < \gamma^{1/4}\sigma_{\rm n}$, then the angles satisfy*

$$\big|\langle \boldsymbol{u}_{\rm ref}, \boldsymbol{u}_1^{(M)}\rangle\big|^2 = 0 + o(1) \quad \textit{in probability,} \tag{4.13}$$

$$\big|\langle \boldsymbol{v}_{\rm ref}, \boldsymbol{v}_1^{(M)}\rangle\big|^2 = 0 + o(1) \quad \textit{in probability.} \tag{4.14}$$

b) *If $\sigma_{\rm ref} > \gamma^{1/4}\sigma_{\rm n}$, then the angles satisfy*

$$\big|\langle \boldsymbol{u}_{\rm ref}, \boldsymbol{u}_1^{(M)}\rangle\big|^2 = \frac{1-\gamma\frac{\sigma_{\rm n}^4}{\sigma_{\rm ref}^4}}{1+\gamma\frac{\sigma_{\rm n}^2}{\sigma_{\rm ref}^2}} + o(1) \quad \textit{in probability,} \tag{4.15}$$

$$\big|\langle \boldsymbol{v}_{\rm ref}, \boldsymbol{v}_1^{(M)}\rangle\big|^2 = \frac{1-\gamma\frac{\sigma_{\rm n}^4}{\sigma_{\rm ref}^4}}{1+\frac{\sigma_{\rm n}^2}{\sigma_{\rm ref}^2}} + o(1) \quad \textit{in probability.} \tag{4.16}$$

In fact, when $\sigma_{\rm ref} = 0$, we know that the singular vectors are uniformly distributed over the unit sphere in $\mathbb{C}^N$ for $\boldsymbol{u}_1^{(M)}$ and in $\mathbb{C}^M$ for $\boldsymbol{v}_1^{(M)}$ [**7, 19**] and therefore

$$\big|\langle \boldsymbol{u}_{\rm ref}, \boldsymbol{u}_1^{(M)}\rangle\big|^2 = \frac{\gamma^{-1}}{M}Z_u + o\big(\frac{1}{M}\big) \quad \text{in distribution,}$$

$$\big|\langle \boldsymbol{v}_{\rm ref}, \boldsymbol{v}_1^{(M)}\rangle\big|^2 = \frac{1}{M}Z_v + o\big(\frac{1}{M}\big) \quad \text{in distribution,}$$

where Z_u and Z_v are two independent random variables with the exponential distribution with mean one.

5. The Evaluation of the Noise Level

5.1. Empirical Estimator. The truncated normalized l^2-norm of the singular values satisfies (4.7). Therefore the truncated normalized l^2-norm of the singular values satisfies

$$M\Big[\frac{1}{M-(1+\gamma^{-1/2})^2}\sum_{j=2}^{M}(\sigma_j^{(M)})^2 - \gamma\sigma_{\rm n}^2\Big] \overset{M\to\infty}{\longrightarrow} b_1 + \sqrt{\gamma}\sigma_{\rm n}^2 Z_0 \text{ in distribution,}$$

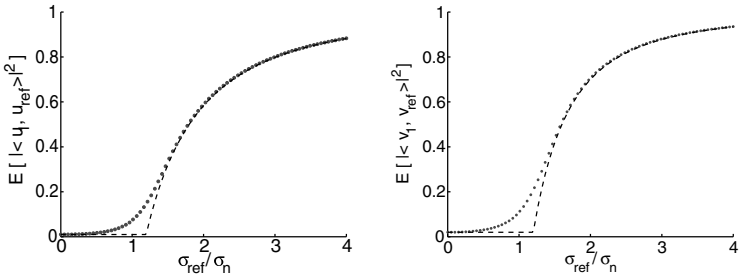

FIGURE 3. Angles between the true and the estimated first left (left picture) and right (right picture) singular vectors. We compare the empirical mean obtained from 10^4 MC simulations (blue dots) with the theoretical formulas given in Proposition 4.3 (dashed lines). Here $N = 100$ and $M = 50$ ($\gamma = 2$).

where Z_0 follows a Gaussian distribution with mean zero and variance one, and the asymptotic bias is

$$b_1 = \sigma_{\rm ref}^2 - \bar\sigma_1^2 + \sigma_{\rm n}^2(1+\gamma^{1/2})^2.$$

Here

$$\bar\sigma_1 = \max\left\{\sigma_{\rm ref}\left(1+(1+\gamma)\frac{\sigma_{\rm n}^2}{\sigma_{\rm ref}^2}+\gamma\frac{\sigma_{\rm n}^4}{\sigma_{\rm ref}^4}\right)^{1/2},\ \sigma_{\rm n}(1+\gamma^{1/2})\right\}$$

is the deterministic leading-order value of the first singular value. The normalization in the truncated l^2-norm has been chosen so that, in the absence of a target, the asymptotic bias is zero:

$$b_1\ |_{\sigma_{\rm ref}=0} = 0.$$

This implies that

$$\hat\sigma_{\rm n}^e := \gamma^{-1/2}\Big[\frac{1}{M-(1+\gamma^{-1/2})^2}\sum_{j=2}^{M}(\sigma_j^{(M)})^2\Big]^{1/2} \tag{5.1}$$

is an empirical estimator of $\sigma_{\rm n}$ with Gaussian fluctuations of the order of $1/M$. This estimator satisfies

$$M\Big[\hat\sigma_{\rm n}^e - \sigma_{\rm n}\Big] \stackrel{M\to\infty}{\longrightarrow} \frac{b_1}{2\gamma\sigma_{\rm n}} + \frac{\sigma_{\rm n}}{2\sqrt{\gamma}}Z_0 \text{ in distribution,}$$

and therefore

$$\hat\sigma_{\rm n}^e = \sigma_{\rm n} + o(\frac{1}{M^{2/3}}) \text{ in probability.} \tag{5.2}$$

The empirical estimator is easy to compute, since it requires the evaluation of the Frobenius norm of the measured matrix $\mathbf{A}$ and the first singular value:

$$\hat\sigma_{\rm n}^e = \gamma^{-1/2}\Big[\frac{\sum_{n=1}^{N}\sum_{m=1}^{M}|A_{nm}|^2 - (\sigma_1^{(M)})^2}{M-(1+\gamma^{-1/2})^2}\Big]^{1/2}. \tag{5.3}$$

5.2. Corrected Empirical Estimator. It is possible to improve the quality of the estimation of the noise level and to cancel the bias of the empirical estimator. Using Proposition 4.2 we can see that the quantity

$$\hat{\sigma}^e_{\mathrm{ref}} = \frac{\hat{\sigma}^e_{\mathrm{n}}}{\sqrt{2}}\left\{\left(\frac{\sigma_1^{(M)}}{\hat{\sigma}^e_{\mathrm{n}}}\right)^2 - 1 - \gamma + \left(\left[\left(\frac{\sigma_1^{(M)}}{\hat{\sigma}^e_{\mathrm{n}}}\right)^2 - 1 - \gamma\right]^2 - 4\gamma\right)^{1/2}\right\}^{1/2} \tag{5.4}$$

is an estimator of σ_{ref}, provided that $\sigma_{\mathrm{ref}} > \gamma^{1/4}\sigma_{\mathrm{n}}$. Therefore, when $\sigma_{\mathrm{ref}} > \gamma^{1/4}\sigma_{\mathrm{n}}$, it is possible to build an improved estimator of the noise variance by removing from the empirical estimator an estimation of the asymptotic bias which is itself based on the empirical estimator $\hat{\sigma}^e_{\mathrm{n}}$. The estimator of the asymptotic bias that we propose to use is

$$\hat{b}^e_1 = \hat{\sigma}^2_{\mathrm{ref}} - (\sigma_1^{(M)})^2 + (\hat{\sigma}^e_{\mathrm{n}})^2(1+\gamma^{1/2})^2, \tag{5.5}$$

and therefore we can propose the following estimator of the noise level σ_{n}:

$$\hat{\sigma}^c_{\mathrm{n}} := \hat{\sigma}^e_{\mathrm{n}} - \frac{\hat{b}^e_1}{2\gamma M \hat{\sigma}^e_{\mathrm{n}}}. \tag{5.6}$$

This estimator satisfies

$$M\left[\hat{\sigma}^c_{\mathrm{n}} - \sigma_{\mathrm{n}}\right] \overset{M\to\infty}{\longrightarrow} \frac{\sigma_{\mathrm{n}}}{2\sqrt{\gamma}} Z_0 \text{ in distribution.}$$

This estimator can only be used when $\hat{\sigma}^e_{\mathrm{ref}} > \gamma^{1/4}\hat{\sigma}^e_{\mathrm{n}}$ and it should then be preferred to the empirical estimator $\hat{\sigma}^e_{\mathrm{n}}$.

5.3. Kolmogorov-Smirnov Estimator. An alternative method to estimate σ_{n} is the approach outlined in [**15**] and applied in [**21**], which consists in minimizing the Kolmogorov-Smirnov distance $\mathcal{D}(\sigma)$ between the observed sample distribution of the $M-K$ smallest singular values of the measured matrix $\mathbf{A}$ and that predicted by theory, which is the deformed quarter circle distribution (4.2) parameterized by σ_{n}. Compared to [**15, 21**] we here introduce a cut-off parameter K that can be chosen by the user. All choices are equivalent in the asymptotic framework $M \to \infty$, but for finite M low values for K give the estimators with minimal variances but with some bias, while large values for K increases the variance but also decays the bias (see Figure 4). We define the new estimator $\hat{\sigma}^K_{\mathrm{n}}$ of σ_{n} as the parameter that minimizes the Kolmogorov-Smirnov distance. After elementary manipulations we find that the Kolmogorov-Smirnov estimator can be defined as

$$\hat{\sigma}^K_{\mathrm{n}} := \operatorname*{argmin}_{\sigma>0} \mathcal{D}_K^{(M)}(\sigma), \tag{5.7}$$

where $\mathcal{D}_K^{(M)}(\sigma)$ is defined by:

$$\mathcal{D}_K^{(M)}(\sigma) := \max_{m=1,\ldots,M-K} \left| G_\gamma\left(\frac{\sigma^{(M)}_{M+1-m}}{\sigma}\right) - \frac{m-1/2}{M}\right| + \frac{1}{2M},$$

G_γ is the cumulative distribution function with density (4.2):

$$G_\gamma(x) = \begin{cases} 0 & \text{if } x \le \gamma^{1/2} - 1, \\ \frac{1}{2} + \frac{\gamma^{1/2}}{\pi}\big(1 - G(x)^2\big)^{1/2} & \\ \quad -\frac{\gamma-1}{\pi}\arctan\Big(\frac{1 - \frac{\gamma+1}{\gamma^{1/2}}G(x)}{(1-G(x)^2)^{1/2}(\frac{\gamma-1}{\gamma^{1/2}})}\Big) & \\ \quad -\frac{\gamma+1}{\pi}\arcsin\big(G(x)\big) & \text{if } \gamma^{1/2} - 1 < x \le \gamma^{1/2} + 1, \\ 1 & \text{if } \gamma^{1/2} + 1 < x, \end{cases}$$

with

$$G(x) = \frac{(1+\gamma) - x^2}{2\gamma^{1/2}}.$$

If $\gamma = 1$, then we have

$$G_1(x) = \begin{cases} 0 & \text{if } x \le 0, \\ \frac{1}{2\pi}\Big(x\sqrt{4-x^2} + 4\arcsin\big(\frac{x}{2}\big)\Big) & \text{if } 0 < x \le 2, \\ 1 & \text{if } 2 < x. \end{cases}$$

5.4. Discussion. The three estimation methods described in the three previous subsections have been implemented and numerical results are reported in Figure 4.

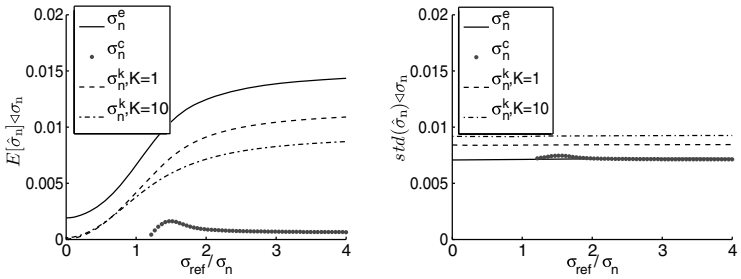

FIGURE 4. Relative bias (left) and standard deviations (right) of different estimators of the noise level. Here $N = 100$ and $M = 50$ ($\gamma = 2$).

As predicted by the asymptotic theory, the variance of the empirical estimator is equivalent to the one of the corrected empirical estimator, and they are smaller than the ones of the Kolmogorov-Smirnov estimator. The bias of the empirical estimator is larger than the bias of the Kolmogorov-Smirnov estimator. The corrected empirical estimator has a very small bias. The variance of the Kolmogorov-Smirnov estimator increases with K, but its bias decreases with increasing K. From these observations it turns out that:
- when $\hat{\sigma}^e_{\rm ref} > \gamma^{1/4}\hat{\sigma}^e_{\rm n}$, then it is recommended to use the corrected empirical estimator (5.6). It is the one that has the minimal bias and the minimal variance amongst all the estimators studied in this paper, but it can only be applied in the regime when the singular value corresponding to the target is outside the deformed quarter-circle distribution of the noise singular values.

- when $\hat{\sigma}^e_{\rm ref} < \gamma^{1/4}\hat{\sigma}^e_{\rm n}$, then it is recommended to use the Kolmogorov-Smirnov estimator (5.7) with $K = 1$. Although its variance is larger than the one of the empirical estimator, its bias is much smaller and, as a result, it is the one that has the minimal quadratic error (sum of the squared bias and of the variance).

The estimator of the noise variance that we will use in the following is accordingly:

$$\hat{\sigma}_{\rm n} = \mathbf{1}_{\hat{\sigma}^e_{\rm ref} \le \gamma^{1/4}\hat{\sigma}^e_{\rm n}} \hat{\sigma}^{K=1}_{\rm n} + \mathbf{1}_{\hat{\sigma}^e_{\rm ref} > \gamma^{1/4}\hat{\sigma}^e_{\rm n}} \hat{\sigma}^c_{\rm n}. \tag{5.8}$$

Its bias and standard deviation are plotted in Figure 5.

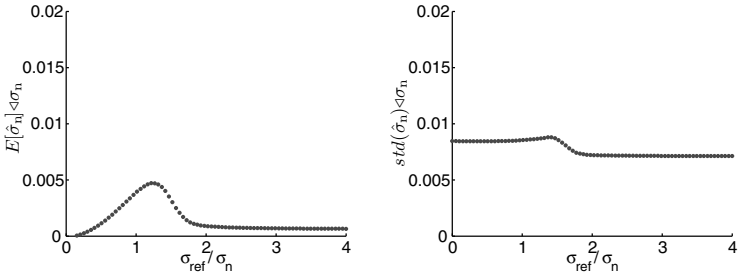

FIGURE 5. Relative bias (left) and standard deviations (right) of the final estimator (5.8) of the noise level. Here $N = 100$ and $M = 50$ ($\gamma = 2$).

6. Detection Test

Consider the response matrix in the presence of measurement noise:

$$\mathbf{A} = \mathbf{A}_0 + \mathbf{W},$$

where $\mathbf{A}_0$ is zero in the absence of a target and equal to (2.4) when there is a target. The matrix $\mathbf{W}$ models additive measurement noise and its complex entries are independent and identically distributed with Gaussian statistics, mean zero and variance $\sigma_{\rm n}^2/M$.

The objective is to propose a detection test for the target. Since we know that the presence of a target is characterized by the existence of a significant singular value, we propose to use a test of the form $R > r$ for the alarm corresponding to the presence of a target. Here R is the quantity obtained from the measured response matrix and defined by

$$R = \frac{\sigma_1^{(M)}}{\hat{\sigma}_{\rm n}}, \tag{6.1}$$

where $\hat{\sigma}_{\rm n}$ is the known value of $\sigma_{\rm n}$, if known, or the estimator (5.8) of $\sigma_{\rm n}$. Here the threshold value r of the test has to be chosen by the user. This choice follows from Neyman-Pearson theory as we explain below. It requires the knowledge of the statistical distribution of R which we give in the following proposition.

PROPOSITION 6.1. *In the asymptotic regime $M \gg 1$ the following statements hold.*

a) *In absence of a target we have*

$$R \simeq 1+\gamma^{1/2}+\frac{1}{2M^{2/3}}\big(1+\gamma^{-1/2}\big)^{1/3}Z_2+o(\frac{1}{M^{2/3}}), \tag{6.2}$$

where Z_2 follows a type-2 Tracy Widom distribution.

b) *In presence of a target:*

b1) *If $\sigma_{\rm ref} > \gamma^{1/4}\sigma_{\rm n}$, then we have*

$$\begin{aligned} R \quad &\simeq \quad \frac{\sigma_{\rm ref}}{\sigma_{\rm n}}\Big(1+(1+\gamma)\frac{\sigma_{\rm n}^2}{\sigma_{\rm ref}^2}+\gamma\frac{\sigma_{\rm n}^4}{\sigma_{\rm ref}^4}\Big)^{1/2} \\ &\quad +\frac{1}{(2M)^{1/2}}\Big(\frac{1-\gamma\frac{\sigma_{\rm n}^4}{\sigma_{\rm ref}^4}}{\big(1+(1+\gamma)\frac{\sigma_{\rm n}^2}{\sigma_{\rm ref}^2}+\gamma\frac{\sigma_{\rm n}^4}{\sigma_{\rm ref}^4}\big)^{1/2}}\Big)^{1/2}Z_0, \end{aligned} \tag{6.3}$$

where Z_0 follows a Gaussian distribution with mean zero and variance one.

b2) *If $\sigma_{\rm ref} = \gamma^{1/4}\sigma_{\rm n}$, then we have*

$$R \simeq 1+\gamma^{1/2}+\frac{1}{2M^{2/3}}\big(1+\gamma^{-1/2}\big)^{1/3}Z_3+o(\frac{1}{M^{2/3}}), \tag{6.4}$$

where Z_3 follows a type-3 Tracy Widom distribution.

b3) *If $\sigma_{\rm ref} < \gamma^{1/4}\sigma_{\rm n}$, then we have (6.2).*

PROOF. We have on the one hand that the truncated normalized l^2-norm of the singular values satisfies (5.2). On the other hand the maximal singular value is described by Proposition 4.2 which gives the desired result by Slutsky's theorem. □

The data (i.e. the measured response matrix) gives the value of the ratio R. We propose to use a test of the form $R > r$ for the alarm corresponding to the presence of a target. The quality of this test can be quantified by two coefficients:
- The false alarm rate (FAR) is the probability to sound the alarm while there is no target:

$$\text{FAR} = \mathbb{P}(R > r_\alpha|\text{ no target }).$$

- The probability of detection (POD) is the probability to sound the alarm when there is a target:

$$\text{POD} = \mathbb{P}(R > r_\alpha|\text{ target }).$$

As is well-known in statistical test theory, it is not possible to find a test that minimizes the FAR and maximizes the POD. However, by the Neyman-Pearson lemma, the decision rule of sounding the alarm if and only if $R > r_\alpha$ maximizes the POD for a given FAR α, provided the threshold is taken to be equal to

$$r_\alpha = 1+\gamma^{1/2}+\frac{1}{2M^{2/3}}\big(1+\gamma^{-1/2}\big)^{1/3}\Phi_{\rm TW2}^{-1}(1-\alpha), \tag{6.5}$$

where $\Phi_{\rm TW2}$ is the cumulative distribution function of the Tracy-Widom distribution of type 2. The computation of the threshold r_α is easy since it depends only on the number of sensors N and M and on the FAR α. We have, for instance, $\Phi_{\rm TW2}^{-1}(0.9) \simeq -0.60$, $\Phi_{\rm TW2}^{-1}(0.95) \simeq -0.23$ and $\Phi_{\rm TW2}^{-1}(0.99) \simeq 0.48$. These values are used in the detection tests whose POD are plotted in Figure 6.

The POD of this optimal test (optimal amongst all tests with the FAR α) depends on the value σ_{ref} and on the noise level σ_{n}. When σ_{ref} is larger than $\gamma^{1/4}\sigma_{\text{n}}$ we find that the POD takes the asymptotic form

$$\text{POD} = \Phi\left(\sqrt{2M}\,\frac{\frac{\sigma_{\text{ref}}}{\sigma_{\text{n}}}\left(1+(1+\gamma)\frac{\sigma_{\text{n}}^2}{\sigma_{\text{ref}}^2}+\gamma\frac{\sigma_{\text{n}}^4}{\sigma_{\text{ref}}^4}\right)^{1/2}-r_\alpha}{\left(\frac{1-\gamma\frac{\sigma_{\text{n}}^4}{\sigma_{\text{ref}}^4}}{\left(1+(1+\gamma)\frac{\sigma_{\text{n}}^2}{\sigma_{\text{ref}}^2}+\gamma\frac{\sigma_{\text{n}}^4}{\sigma_{\text{ref}}^4}\right)^{1/2}}\right)^{1/2}}\right), \tag{6.6}$$

where Φ is the cumulative distribution function of the normal distribution with mean zero and variance one. The theoretical test performance improves very rapidly with M once $\sigma_{\text{ref}} > \gamma^{1/4}\sigma_{\text{n}}$. This result is indeed valid as long as $\sigma_{\text{ref}} > \gamma^{1/4}\sigma_{\text{n}}$. When $\sigma_{\text{ref}} < \gamma^{1/4}\sigma_{\text{n}}$, so that the target is buried in noise (more exactly, the singular values corresponding to the target are buried into the deformed quarter-circle distribution of the other singular values), then we have POD $= 1-\Phi_{\text{TW2}}\big(\Phi_{\text{TW2}}^{-1}(1-\alpha)\big) = \alpha$. In the critical case in which $\sigma_{\text{ref}} = \gamma^{1/4}\sigma_{\text{n}}$ then we have POD $= 1-\Phi_{\text{TW3}}\big(\Phi_{\text{TW2}}^{-1}(1-\alpha)\big)$. We have for instance $\Phi_{\text{TW3}}\big(\Phi_{\text{TW2}}^{-1}(0.9)\big) \simeq 0.49$, $\Phi_{\text{TW3}}\big(\Phi_{\text{TW2}}^{-1}(0.95)\big) \simeq 0.62$, and $\Phi_{\text{TW3}}\big(\Phi_{\text{TW2}}^{-1}(0.99)\big) \simeq 0.82$.

The POD of the test (6.1) calibrated for different values of the FAR is plotted in Figure 6. One can observe that the calibration with r_α gives the desired FAR and that the POD rapidly goes to one when the singular value σ_{ref} of the target is larger than $\gamma^{1/4}\sigma_{\text{n}}$. Furthermore, the use of the estimator (5.8) for the noise level σ_{n} is also very efficient in that we get almost the same FAR and POD with the true value σ_{n} as with the estimator $\hat{\sigma}_{\text{n}}$.

Remark: The previous results were obtained by an asymptotic analysis assuming that M is large and σ_{ref} and σ_{n} are of the same order. In the case in which σ_{ref} is much larger than σ_{n}, then the proposed test has a POD of 100%. In the case in which σ_{ref} is much smaller than σ_{n}, then it is not possible to detect the target from the singular values of the response matrix and the proposed test has a POD equal to the FAR (as shown above, this is the case when $\sigma_{\text{ref}} < \gamma^{1/4}\sigma_{\text{n}}$).

7. Target Localization and Reconstruction

In this section we would like to present simple and robust way to localize the target and reconstruct its properties once the detection test has passed. By simple we mean that we will only use the first singular value and singular vector of the response matrix, and by robust we mean a procedure that allows for estimations with bias and variance as small as possible.

7.1. Localization. A standard imaging functional is the MUSIC functional defined by

$$\mathcal{I}_{\text{MUSIC}}(\boldsymbol{x}) \;:=\; \big\|\boldsymbol{u}(\boldsymbol{x}) - \big({\boldsymbol{u}_1^{(M)}}^\dagger \boldsymbol{u}(\boldsymbol{x})\big)\boldsymbol{u}_1^{(M)}\big\|^{-1/2} = \big(1-\big|\boldsymbol{u}(\boldsymbol{x})^\dagger \boldsymbol{u}_1^{(M)}\big|^2\big)^{-1/2},$$

where $\boldsymbol{u}(\boldsymbol{x})$ is the normalized vector of Green's functions (2.8). In fact it is a nonlinear function of a weighted subspace migration functional:

$$\mathcal{I}_{\text{SM}}(\boldsymbol{x}) = 1 - \mathcal{I}_{\text{MUSIC}}(\boldsymbol{x})^{-2}\big|\boldsymbol{u}(\boldsymbol{x})^\dagger \boldsymbol{u}_1^{(M)}\big|^2. \tag{7.1}$$

In the absence of noise the MUSIC functional presents a peak with amplitude one at $\boldsymbol{x} = \boldsymbol{x}_{\text{ref}}$. In the presence of noise the peak of the MUSIC functional is slightly

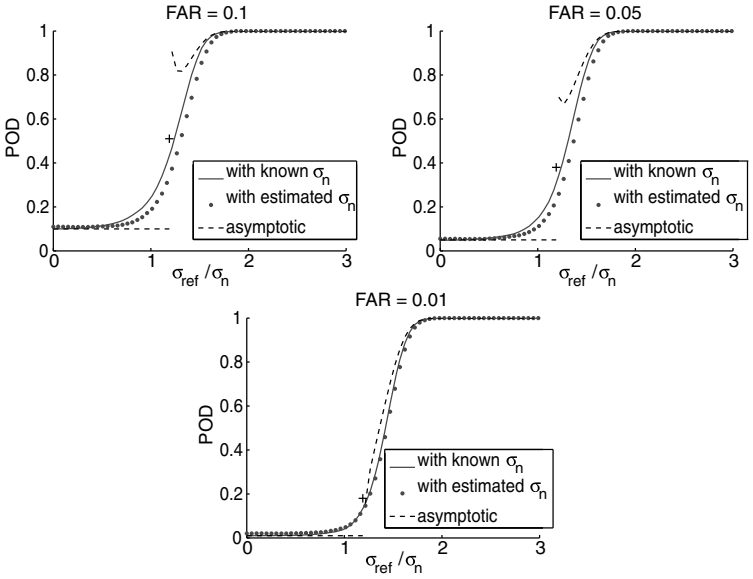

FIGURE 6. Probability of detection for the detection test calibrated with the threshold values r_α with $\alpha = 0.1$ (top left), $\alpha = 0.05$ (top right), and $\alpha = 0.01$ (bottom). Here $N = 100$ and $M = 50$. The blue solid and dotted lines correspond to the results of 10^4 MC simulations, in which the noise level is known (solid) or estimated by (5.8) (dotted). The dashed lines are the FAR desired in the absence of a target, that should be obtained when $\sigma_{\rm ref} = 0$, and the asymptotic formula (6.6), that should be obtained for $\sigma_{\rm ref} > \gamma^{1/4}\sigma_{\rm n}$ (in the regime $M \gg 1$). The crosses are the theoretical POD for $\sigma_{\rm ref} = \gamma^{1/4}\sigma_{\rm n}$.

affected. By Proposition 4.3 the theoretical value at $\boldsymbol{x} = \boldsymbol{x}_{\rm ref}$ is deterministic in the regime $M \gg 1$ and given by

$$\mathcal{I}_{\rm SM}(\boldsymbol{x}_{\rm ref}) = c_u,$$

where c_u is the theoretical angle between the left singular vector $\boldsymbol{u}_{\rm ref}$ of the unperturbed matrix $\mathbf{A}_0$ and the left singular vector $\boldsymbol{u}_1^{(M)}$ of the measured response matrix $\mathbf{A}$:

$$c_u = \begin{cases} \dfrac{1-\gamma\frac{\sigma_{\rm n}^4}{\sigma_{\rm ref}^4}}{1+\gamma\frac{\sigma_{\rm n}^2}{\sigma_{\rm ref}^2}} & \text{if } \sigma_{\rm ref} > \gamma^{1/4}\sigma_{\rm n}, \\ 0 & \text{if } \sigma_{\rm ref} < \gamma^{1/4}\sigma_{\rm n}. \end{cases}$$

Therefore, provided the detection test has passed, which means that the target singular value is larger than the noise singular values, the MUSIC algorithm gives a robust and simple way to estimate the position of the reflector. The estimator of $\boldsymbol{x}_{\rm ref}$ that we propose is

$$\hat{\boldsymbol{x}}_{\rm ref} := \operatorname*{argmin}_{\boldsymbol{x}} \mathcal{I}_{\rm SM}(\boldsymbol{x}). \tag{7.2}$$

Note that more complex and computationally expensive algorithms (using reverse-time migration) can improve the quality of the estimation as shown in [**2**].

7.2. Reconstruction. Using Proposition 4.2 we can see that the quantity

$$\hat{\sigma}_{\mathrm{ref}} = \frac{\hat{\sigma}_{\mathrm{n}}}{\sqrt{2}}\Big\{\Big(\frac{\sigma_1^{(M)}}{\hat{\sigma}_{\mathrm{n}}}\Big)^2 - 1 - \gamma + \Big(\Big[\Big(\frac{\sigma_1^{(M)}}{\hat{\sigma}_{\mathrm{n}}}\Big)^2 - 1 - \gamma\Big]^2 - 4\gamma\Big)^{1/2}\Big\}^{1/2} \tag{7.3}$$

is an estimator of σ_{ref}, provided that $\sigma_{\mathrm{ref}} > \gamma^{1/4}\sigma_{\mathrm{n}}$. In practice, if the detection test passes, then this implies in particular that we are in this case provided that $r_\alpha \geq 0$. From (2.6) we can therefore estimate the scattering amplitude ρ_{ref} of the inclusion by

$$\hat{\rho}_{\mathrm{ref}} = \frac{c_0^2}{\omega^2}\Big(\sum_{n=1}^{N}|\hat{G}(\omega,\hat{\boldsymbol{x}}_{\mathrm{ref}},\boldsymbol{y}_n)|^2\Big)^{-1/2}\Big(\sum_{m=1}^{M}|\hat{G}(\omega,\hat{\boldsymbol{x}}_{\mathrm{ref}},\boldsymbol{z}_m)|^2\Big)^{-1/2}\hat{\sigma}_{\mathrm{ref}}, \tag{7.4}$$

with $\hat{\sigma}_{\mathrm{ref}}$ the estimator (7.3) of σ_{ref} and $\hat{x}_{\mathrm{ref}}$ is an estimator of the position of the inclusion. This estimator is not biased asymptotically because it compensates for the level repulsion of the first singular value due to the noise.

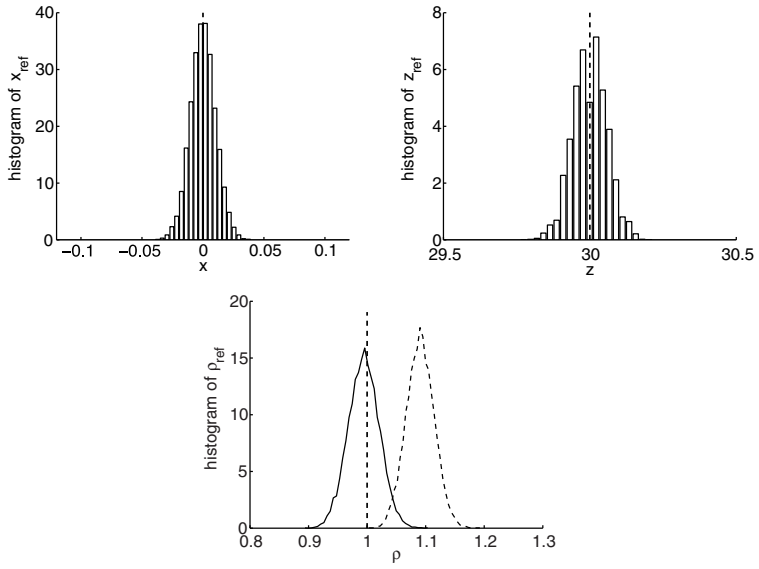

FIGURE 7. Top left: Histogram of the estimated cross-range position $\hat{x}_{\mathrm{ref}}$ given by (7.2). Top right: Histogram of the estimated range position $\hat{z}_{\mathrm{ref}}$ given by (7.2). Bottom: Histogram of the estimated scattering amplitude $\hat{\rho}_{\mathrm{ref}}$ given by (7.4) (solid lines) or $\hat{\rho}^e_{\mathrm{ref}}$ given by (7.5) (dashed lines). Here $\sigma_{\mathrm{n}} = \sigma_{\mathrm{ref}}/4$.

7.3. Numerical Simulations. We consider the following numerical set-up: the wavelength is equal to one (i.e. $\omega = 2\pi$, $c_0 = 1$). There is one reflector with scattering amplitude $\rho_{\mathrm{ref}} = 1$, located at $\boldsymbol{x}_{\mathrm{ref}} = (0, 0, 30)$. We consider a linear array of $N = 100$ transducers located at half-a-wavelength apart on the line from $(-25, 0, 0)$ to $(25, 0, 0)$. Each transducer is used as a receiver, but only one of two

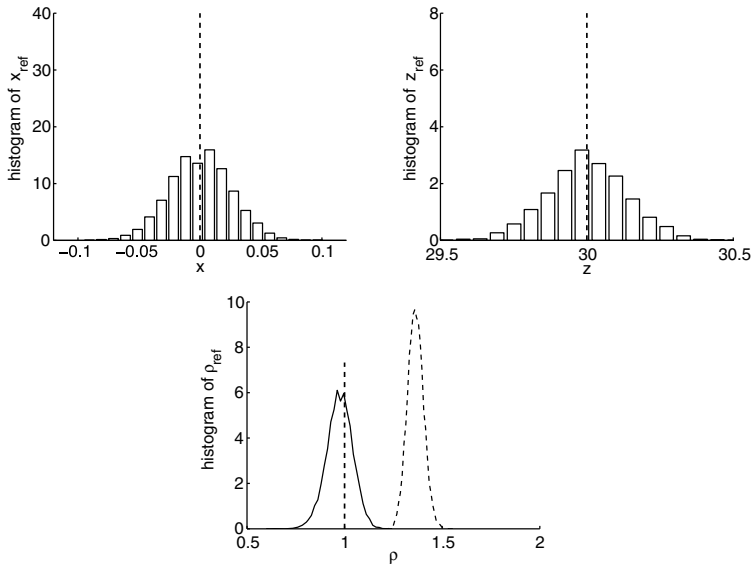

FIGURE 8. The same as in Figure 7, but here $\sigma_{\rm n} = \sigma_{\rm ref}/2$.

is used as a source (therefore, $M = 50$ and $\gamma = 2$). The noise level is $\sigma_{\rm n} = \sigma_{\rm ref}/4$ or $\sigma_{\rm ref}/2$, where $\sigma_{\rm ref}$ is the singular value associated to the reflector (given by (2.6)).

We have carried out a series of 10^4 MC simulations. The results are reported in Figure 7 (for $\sigma_{\rm n} = \sigma_{\rm ref}/4$) and in Figure 8 (for $\sigma_{\rm n} = \sigma_{\rm ref}/2$):

- the reflector is always detected (as shown in Figure 6 the POD is almost one when $\sigma_{\rm ref} \geq 2\sigma_{\rm ref}$).

- the estimator $\hat{\boldsymbol{x}}_{\rm ref}$ defined by (7.2) of the position of the reflector has good properties. The histograms of the estimated positions $\hat{\boldsymbol{x}}_{\rm ref} = (\hat{x}_{\rm ref}, 0, \hat{z}_{\rm ref})$ are plotted in Figures 7-8 (left and center).

- the estimator $\hat{\rho}_{\rm ref}$ defined by (7.4) of the scattering amplitude has a very small bias because it uses the inversion formula (7.3) which compensates for the level repulsion of the first singular value. We plot in Figures 7-8 (right) the histogram of the estimated scattering amplitude and we compare with the empirical estimator

$$\hat{\rho}^e_{\rm ref} = \frac{c_0^2}{\omega^2}\Big(\sum_{n=1}^{N} |\hat{G}(\omega, \hat{\boldsymbol{x}}_{\rm ref}, \boldsymbol{y}_n)|^2\Big)^{-1/2}\Big(\sum_{m=1}^{M} |\hat{G}(\omega, \hat{\boldsymbol{x}}_{\rm ref}, \boldsymbol{z}_m)|^2\Big)^{-1/2}\sigma_1^{(M)}, \tag{7.5}$$

which has a large bias.

References

[1] H. Ammari, J. Garnier, H. Kang, W.-K. Park, and K. Sølna, Imaging schemes for perfectly conducting cracks, SIAM J. Appl. Math., 71 (2011), 68–91.

[2] H. Ammari, J. Garnier, and K. Sølna, A statistical approach to target detection and localization in the presence of noise, to appear in Waves in Random and Complex Media.

[3] H. Ammari and H. Kang, *Reconstruction of Small Inhomogeneities from Boundary Measurements*, Lecture Notes in Mathematics, Volume 1846, Springer-Verlag, Berlin, 2004.

[4] H. Ammari and H. Kang, *Polarization and Moment Tensors: with Applications to Inverse Problems and Effective Medium Theory*, Applied Mathematical Sciences, Vol. 162, Springer-Verlag, New York, 2007.

[5] H. Ammari, M. Vogelius, and D. Volkov, Asymptotic formulas for perturbations in the electromagnetic fields due to the presence of inhomogeneities of small diameter II. The full Maxwell equations, J. Math. Pures Appl., 80 (2001), 769–814.
[6] H. Ammari and D. Volkov, The leading-order term in the asymptotic expansion of the scattering amplitude of a collection of finite number of dielectric inhomogeneities of small diameter, International Journal for Multiscale Computational Engineering, 3 (2005), 149–160.
[7] T. W. Anderson, Asymptotic theory of principal component analysis, Ann. Math. Statist., 34 (1963), 122–148.
[8] B. Angelsen, *Ultrasound Imaging. Waves, Signals and Signal Processing*, Emantec, Trondheim, 2000.
[9] A. Aubry and A. Derode, Random matrix theory applied to acoustic backscattering and imaging in complex media, Phys. Rev. Lett. 102 (2009), 084301.
[10] A. Aubry and A. Derode, Singular value distribution of the propagation matrix in random scattering media, Waves Random Complex Media 20 (2010), 333-363.
[11] A. Aubry and A. Derode, Detection and imaging in a random medium: A matrix method to overcome multiple scattering and aberration, J. Appl. Physics 106 (2009), 044903.
[12] J. Baik, G. Ben Arous, and S. Péché, Phase transition of the largest eigenvalue for nonnull complex sample covariance matrices, Ann. Probab., 33 (2005), 1643–1697.
[13] J. Baik, R. Buckingham, and J. DiFranco, Asymptotics of Tracy-Widom distributions and the total integral of a Painlevé II function, Communications in Mathematical Physics, 280 (2008), 463–497.
[14] M. Capitaine, C. Donati-Martin, and D. Féral, Central limit theorems for eigenvalues of deformations of Wigner matrices, arXiv:0903.4740.
[15] L. Györfi, I. Vajda, and E. Van Der Meulen, Minimum Kolmogorov distance estimates of parameters and parametrized distributions, Metrika, 43 (1996), 237–255.
[16] J. Hadamard, Résolution d'une question relative aux déterminants, Bull. Sci. Math., 17 (1893), 30–31.
[17] I. M. Johnstone, On the distrbution of the largest eigenvalue in principal components analysis, Ann. Statist., 29 (2001), 295–327.
[18] V. A. Marcenko and L. A. Pastur, Distributions of eigenvalues of some sets of random matrices, Math. USSR-Sb., 1 (1967), 507–536.
[19] R. J. Muirhead, *Aspects of Multivariate Statistical Theory*, Wiley, New York, 1982.
[20] J. Seberry, B. J. Wysocki, and T. A. Wysocki, On some applications of Hadamard matrices, Metrika, 62 (2005), 221–239.
[21] A. Shabalin and A. Nobel, Reconstruction of a low-rank matrix in the presence of Gaussian noise, arXiv:1007.4148v1.
[22] S. Stergiopoulos, *Advanced Signal Processing Handbook: Theory and Implementation for Radar, Sonar, and Medical Imaging real-time systems*, CRC Press LLC, Boca Raton, 2001.

Laboratoire de Probabilités et Modèles Aléatoires & Laboratoire Jacques-Louis Lions site Chevaleret, Université Paris VII, 75205 Paris Cedex 13, France
E-mail address: garnier@math.jussieu.fr